Pakistan Veterinary Journal

ISSN: 0253-8318 (PRINT), 2074-7764 (ONLINE)
DOI: 10.29261/pakvetj/2026.151

RESEARCH ARTICLE

Preparation and Functional Verification of Polyclonal Antibodies Targeting IRF8 Protein in Broilers with Pulmonary Hypertension Syndrome

Sufang Cheng[1,2#], liling Liu[1#], Xin Liu[1], Xiaoquan Guo[1], Xiaona Gao[1], Pei Liu[1], Guoliang Hu[1], Xiaoqin Hu[3*] and Ping Liu[1*]

[1]Jiangxi Provincial Key Laboratory for Animal Health, Institute of Animal Population Health, College of Animal Science and Technology, Jiangxi Agricultural University, Nanchang 330045, PR China; [2]Jiangxi Biological Vocational College, Nanchang, Jiangxi 330200, China; [3]Jiangxi Agricultural Engineering Vocational colleg, Zhangshu, Jiangxi 331200, China
[#]These authors contributed equally to this study and shared the first authorship.
*Corresponding author: 125885597@qq.com (XH); pingliujx@163.com (PL)

ARTICLE HISTORY (25-1230)

Received: December 04, 2025
Revised: April 29, 2026
Accepted: May 10, 2026
Published online: June 10, 2026

Key words:
Ascites syndrome
IRF8
Polyclonal antibody
Pulmonary arterial hypertension

ABSTRACT

One of the core pathological changes in Broiler Ascites Syndrome (AS) is compensatory hypertrophy of the right ventricle induced by pulmonary hypertension. IRF8 (Interferon Regulatory Factor 8) acts as a repressor regulator of pulmonary vascular remodeling and cardiac hypertrophy, playing an essential role in both pulmonary and cardiovascular remodeling. Currently, few direct studies have been conducted to explore the correlation between the IRF8 gene and the pathogenic mechanism of broiler ascites syndrome. To explore the important role of IRF8 in AS, this study conducted a bioinformatics analysis of IRF8 and employed recombinant gene technology, protein purification, and immunohistochemistry to obtain mouse anti-chicken IRF8 antibodies. The expression of IRF8 was further validated in animals, including broilers and ascites broilers. The results demonstrated that this study successfully prepared and purified a rabbit anti-chicken IRF8 polyclonal antibody. The antibody's titer, specificity, and reactivity were validated using ELISA, Western blot, and indirect immunohistochemistry. The differential expression of IRF8 in key tissues of affected chickens with AS was also analyzed. This polyclonal antibody serves as a reliable tool for detecting, localizing, and studying the function of IRF8. Additionally, it provides an experimental foundation and new insights into understanding the regulatory mechanisms of IRF8 in AS in broilers, aiding in the precise prevention and control of the disease. They further explained the role of IRF8 in pulmonary vascular remodeling during broiler ascites syndrome, thereby establishing a theoretical foundation for investigating the underlying mechanism of IRF8 in this syndrome, identifying potential diagnostic markers, and developing targeted therapies.

To Cite This Article: Cheng S, Liu I, Liu X, Guo X, Gao X, Liu P, Hu G, Hu X and Liu P, 2026. Preparation and functional verification of polyclonal antibodies targeting IRF8 protein in broilers with pulmonary hypertension syndrome. Pak Vet J, 46(6): 1595-1602. http://dx.doi.org/10.29261/pakvetj/2026.151

INTRODUCTION

AS is a metabolic disease related to pulmonary artery remodeling, also known as pulmonary hypertension syndrome (PHS). It imposes substantial economic losses on global poultry farming (Daneshyar *et al.,* 2009; Li *et al.,* 2022). A multitude of studies have demonstrated that pulmonary hypertension will changes the structure and function of pulmonary artery endothelial cells, changes the permeability of endothelial cells, and even damages the cell membrane and organelle membrane, resulting in vascular endothelial injury and stimulation of smooth muscle contraction of the vascular wall, media thickening, and duct stenosis (Shi *et al.,* 2017), eventually leading to serious damage to the heart and lung function (Zohrabi *et al.,* 2024; Habibian *et al.,* 2025). Interferon regulatory factor 8 (IRF8), which is also denominated as interferon consensus sequence-binding protein, triggers a systemic inflammatory response by activating "inflammatory" macrophages in the lungs. The persistent inflammatory response is the fundamental driving force behind vascular remodeling, thereby contributing to the onset and progression of ascites-associated pulmonary hypertension in broilers (Cytlak *et al.,* 2020; Liang *et al.,* 2023). Few

studies have confirmed that IRF8 plays an important role in immune cell differentiation and innate immunity. IRF8 is also involved in the formation of carotid plaque and increases the thickness of the carotid intima and media, suggesting that IRF8 may play an important role in the phenotypic transformation of VSMC (vascular smooth muscle cell) and the formation of neointima (Liu *et al.,* 2017). Furthermore, IRF8 has been found to be a negative regulator of pulmonary vascular remodeling and cardiac hypertrophy both in vivo and in vitro (Peng *et al.,* 2024).

At present, there are few studies on chicken IRF8 protein and a lack of antibodies. Therefore, we aimed to prepare IRF8 polyclonal antibodies, prokaryotic expression, and protein purification. This provides a basis for studying pulmonary artery remodeling associated with broiler ascites syndrome and the development of IRF8 gene drugs targeting broiler AS prevention and treatment, which has clinical value in reducing the occurrence of broiler AS.

MATERIALS AND METHODS

The Ethics Committee of the Institutional Animal Care and Use Committee at JXAU in China approved the institutional and governmental regulations governing the ethical use of animals.

Bioinformatics analysis of IRF8: The transmembrane topology of IRF8 was analyzed using the TMHMM Server v2.0, and its hydrophobicity/hydrophilicity profiles were characterized using the ProtParam tool. Signal peptide motifs were identified using SignalP 3.0. All amino acid sequences were retrieved from the NCBI GenBank (Gene ID: 396385). For JAZF1 protein analysis, secondary structural features and immunogenic epitopes (T/B cell epitopes) were predicted using the Protean module in DNAStar 7.1.

Experimental Animals: A total of 30 white-feathered broilers were subjected to random grouping, being divided into a control group and an ascites group with 15 individuals in each group. The experimental animals were allowed to move freely and had unrestricted access to the food. The control group was housed under optimal environmental conditions, where the ambient temperature was maintained at around 25°C and the relative humidity at approximately 45%. The birds had *ad libitum* access to clean drinking water and a basal diet throughout the experiment. On the contrary, the ascites group was provided with a customized diet supplemented with 3% lard and 4% fish meal. The broilers were provided with purified drinking water supplemented with 0.3% sodium chloride, and the temperature of their rearing environment was maintained at 4°C. An animal model of AS was developed in a low-temperature and high-energy environment. On the 30th day, all experimental animals were euthanized. The pulmonary arteries of each broiler were collected into 1.5 milliliter EP tubes and stored at -80°C for future experiments.

DNA extraction and PCR amplification: Following the manufacturer's protocol, RNA was extracted from the pulmonary artery tissue in a low-temperature environment. Then synthesized via reverse transcription using a specified kit (TransGen Biotech, Beijing, China). The detection primers used were IRF8-F: 5'-TCTTTGCCCCTGGTGAATGG-3' and IRF8-R: 5'-CCCAAGCTTTCATAAGTGTG -3'. Each PCR reaction was prepared in a 20μL volume, consisting of 10μL of 2×Taq Master Mix, 1μL of each primer (at a concentration of 2μmol/L per primer), 1μL of the extracted DNA template, and 7μL of ddH_2O. The thermal cycling program initiated with an initial denaturation step at 95℃ for 3 minutes, followed by 35 amplification cycles consisting of denaturation at 94℃ for 30s, annealing for 30s, and extension at 72℃ for 1 minute. A final extension step was conducted at 72℃ for 10 minutes using a thermal cycler, and the resultant PCR products were verified via 1% agarose gel electrophoresis.

IRF8 Cloning/Expression Vector Construction and Purification: In this research, the purified amplified products of the target gene were inserted into the pEASY®-T3 cloning vector following the provided instructions, and then introduced into Trans5α receptor cells. The cells were evenly spread on an LB solid culture plate (with ampicillin at a concentration of 100μg/mL) and incubated upside down at 37℃ for 12-24h. Subsequently, a single bacterial colony was selected for PCR amplification, and the positive colonies identified by PCR were subjected to sequencing analysis. Following gene sequencing verification, the target recombinant plasmid and empty pET-32a(+) vector were successfully purified. The purified samples were incubated at 37°C for 12–24h. Subsequently, both the positive plasmid and pET-32a(+) vector were subjected to double digestion using Hind III restriction enzyme. Under the catalysis of T4 DNA ligase, the IRF8 insert fragment was directionally cloned into the pET-32a expression vector via restriction enzyme digestion, followed by transformation into Transetta (DE3) competent cells. The resulting positive recombinant plasmid was designated as IRF8-pET-32a.

Induction of recombinant protein expression was performed: LB bacterial broth was utilized as the culture medium for recombinant protein production. When the optical density of the bacterial culture at 600 nm (OD_{600}) reached the range of 0.5–0.8, 1mM isopropyl β-D-thiogalactoside (IPTG) was supplemented into the LB medium. Subsequently, the culture was incubated with shaking at 37℃ and 180 rpm for 10 hours to induce recombinant protein expression. Subsequently, all bacterial suspensions were subjected to centrifugation to collect the resulting precipitates. The precipitates were then sonicated and resuspended. After an additional centrifugation step, the expression pattern of the recombinant protein was evaluated via SDS-PAGE combined with Coomassie Brilliant Blue R-250 staining, with both the culture supernatant and bacterial pellet subjected to analysis. Purification of the target recombinant protein was implemented using a standardized Sephacryl chromatography column. (supplied by Sangong Biotechnology, Shanghai, China), and the ideal eluent concentration was determined. Elution was performed using buffers containing imidazole at concentrations of 100, 200, 300, 400, and 500 mM. The effectiveness of each elution step was evaluated using SDS-PAGE coupled with Coomassie Brilliant Blue R-250 staining.

Preparation of an Antibody Against the IRF8 Protein: Mice were selected as the immunized animals for the conduct of this experiment. Before immunization, blood was collected from the tail to isolate serum, which served as a negative control. A mixture was prepared by emulsifying equal amounts of fuchsin complete adjuvant using the recombinant protein at a concentration of 0.05mg/mL. Additionally, *Poria cocos* polysaccharide at a concentration of 4mg/mL was added to the recombinant protein before emulsification. An equal-volume mixture of fuchsin complete adjuvant and recombinant protein at a concentration of 0.05mg/mL was subjected to thorough emulsification. The emulsified mixture was administered to each mouse via three subcutaneous injections. Subsequently, the mice were administered booster immunizations in different areas. Booster immunizations were administered at 10-day intervals. For booster immunization, a 1:1 volume mixture of recombinant IRF8 protein and Freund's incomplete adjuvant was prepared, and two rounds of booster injections were implemented. At 10 days post the third booster, blood was sampled from the ear artery of the experimental animals, followed by centrifugation at 4500×g for 3 min to isolate the target antiserum.

Polyclonal antibody titer determination: The recombinant IRF8 protein was used to coat 96-well plates at the optimal antigen coating concentration of 2.5μg/mL, followed by overnight incubation at 4°C. After coating, the 96-well plates were washed three times with PBST buffer and then blocked with 5% skim milk for 2 hours at 37°C. Subsequently, the negative and positive mouse anti-IRF8 sera were subjected to serial dilution at concentrations starting from 100, 200, 400, 800, 1600, 3200, 6400, 12,800, 25,600, 51,200, 102,400, 204,800, and 409,600 times and then added to the 96-well plate, incubated at 37°C for 1h. Subsequently, the plate was washed three times with PBST and incubated with a secondary antibody (goat anti-mouse IgG-HRP, diluted 1:5000) at 37°C, incubated for lh. Finally, a soluble TMB chromogenic solution was added to each well, and the plate was incubated in the dark for 20 minutes to allow color development. The chromogenic reaction was terminated by adding diluted concentrated sulfuric acid, and the absorbance value of each well was measured at a wavelength of 450nm using a microplate reader.

Western blotting: Total protein extraction from tissue samples was quantified using the BCA assay. Subsequently, protein samples underwent 12% SDS-PAGE electrophoresis at 120V for 2h. Protein transfer was performed via wet blotting onto PVDF membranes for 40 minutes. Membrane blocking was implemented with a 5% skimmed milk solution at ambient temperature for a duration of 120 minutes. The incubation of the primary antibody was conducted using mouse anti-chicken IRF8 antibody at a dilution ratio of 1:1000, with the reaction maintained at 4°C for 12h. In the secondary detection step, HRP-conjugated goat anti-mouse IgG (H+L) antibody, which was diluted to 1:5000, was added and incubated for 40 minutes under room temperature conditions. Eventually, protein detection was accomplished by means of a ChemiDoc chemiluminescence imaging system.

Immunohistochemistry analysis: Paraffin sections were cut and dewaxed. After antigen retrieval was completed, the tissue sections were subjected to blocking treatment with goat serum for a period of 30 minutes. Following this, the slides were subjected to overnight incubation at 4℃ with both anti-IRF8 positive serum and anti-IRF8 negative serum. Afterward, the slides underwent three washes with PBST and were then treated with a goat anti-mouse IgG solution for 50min at room temperature. Slides underwent hematoxylin counterstaining to visualize nuclei, and the negative controls were established through the primary antibody.

Statistical analysis: Statistical analyses were performed with the aid of SPSS 25 software. Comparisons between two distinct groups were implemented via independent samples t-tests, while one-way ANOVA was employed for data comparisons among multiple groups. Continuous variables are presented as mean ± standard deviation (SD), and the significance thresholds are defined as follows: $P<0.05$, $*P<0.01$, $**P<0.001$.

RESULTS

Bioinformatics analysis of the IRF8 gene: Bioinformatic analysis predicted that IRF8 comprises 1278 amino acids with distinct physicochemical properties. The results of the analysis indicated that the maximum hydrophobicity score of the IRF8 protein was -0.500, while its highest hydrophilicity value reached 2.267. The hydrophilicity prediction results indicate that the value exceeds the established threshold, confirming that the IRF8 protein is hydrophilic, as depicted in Fig. 1(A). TMHMM analysis further demonstrated the absence of significant transmembrane domains within the IRF8 amino acid sequence as shown in Fig.1(B). Additionally, signal peptide prediction suggests the presence of a signal peptide, indicating that IRF8 may function as a secretory protein as shown in Fig.1(C). Phosphorylation, as a gene expression regulatory protein, is one of the important characteristics of a protein and is closely related to the function of the protein. There were multiple phosphorylation sites of the IRF8 protein as shown in Fig.1(D), of which serine (Ser), threonine (Thr), and tyrosine (Tyr) had 28, 15, and 16 sites, respectively. There were two N-glycosylation reform sites at 87(0.1851) NITI and 126—NSSS, indicating that these sites may be encompassed by more than one peptide as shown in Fig.1(E). Utilizing AlphaFold 3's diffusion-based architecture, we determined the 3D structure of chicken IRF8 protein with high accuracy as shown in Fig.1(F).

PCR amplification, cloning, and identification of the IRF8 gene: The target gene of IRF8 was amplified by PCR using the cDNA obtained by reverse transcription of pulmonary artery RNA of broiler chickens as shown in Fig. 2(A). After purification, the products were recovered and cloned into the pET-32a (+) vector, and then double enzyme digestion was performed to identify the pET-32a (+) recombinant plasmid. A target band of about 714bp was detected, indicating that the recombinant plasmid was successfully constructed. At the same time, the same

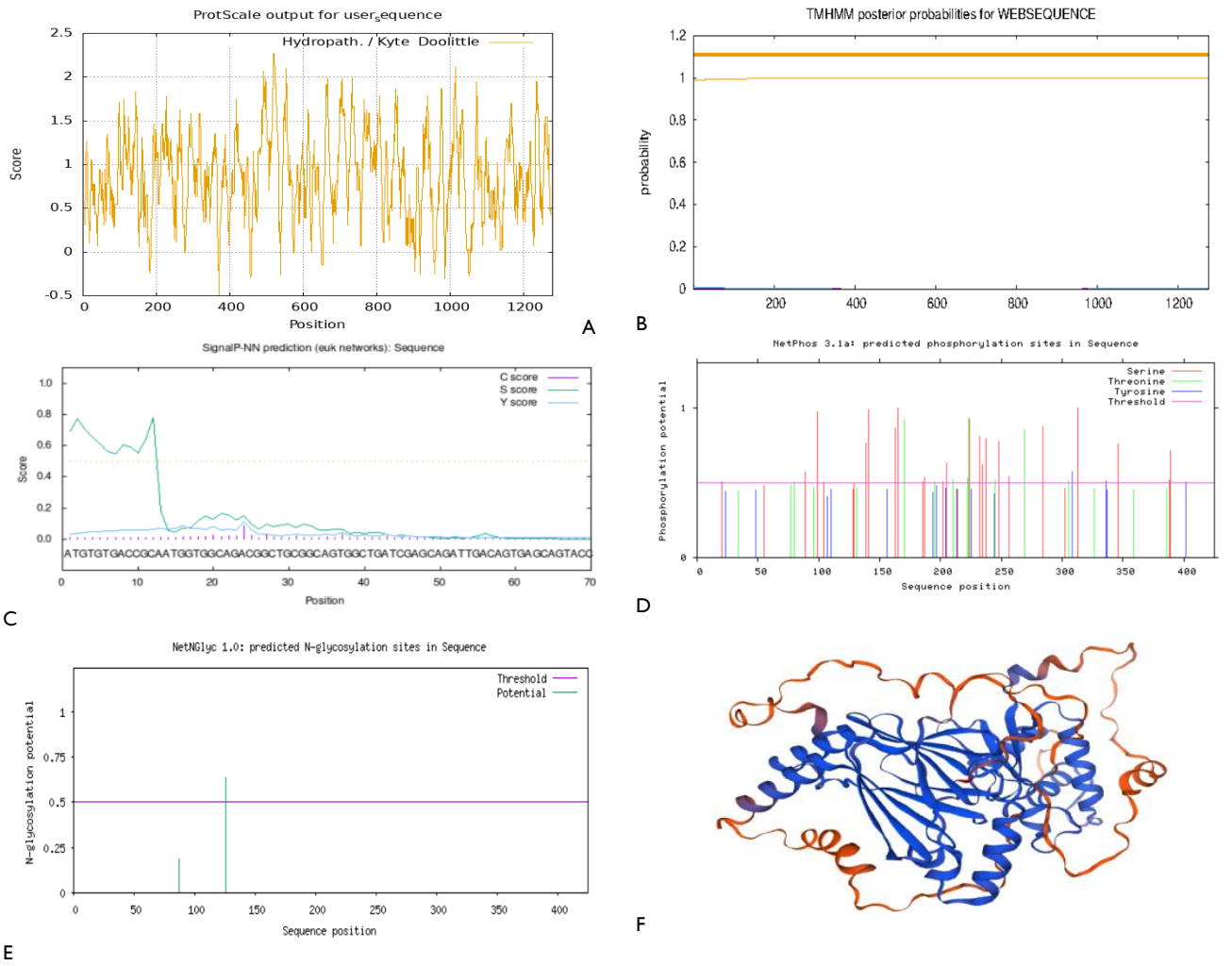

Fig.1: (A) Prediction of chicken IRF8 protein hydrophilicity. (B) Transmembrane domain of IRF8 protein. The dark yellow line represents the FSHβ protein, the yellow line below represents the outer cell membrane, and the blue line represents the inner cell membrane. (C) Prediction of the signal peptide of the IRF8 protein. The four curves comprehensively show the locations of possible cleavage sites and signal peptide regions. (D) Phosphorylation site of IRF8 protein. Serine (E) Prediction of glycosylation sites. The potential glycosylation sites are shown by green lines, while threshold is indicated by purple lines. (F) Tertiary structure of IRF8 protein. Red color indicates α-helix, yellow indicates β-turning angle, green indicates Random coil, and blue indicates transmembrane region.

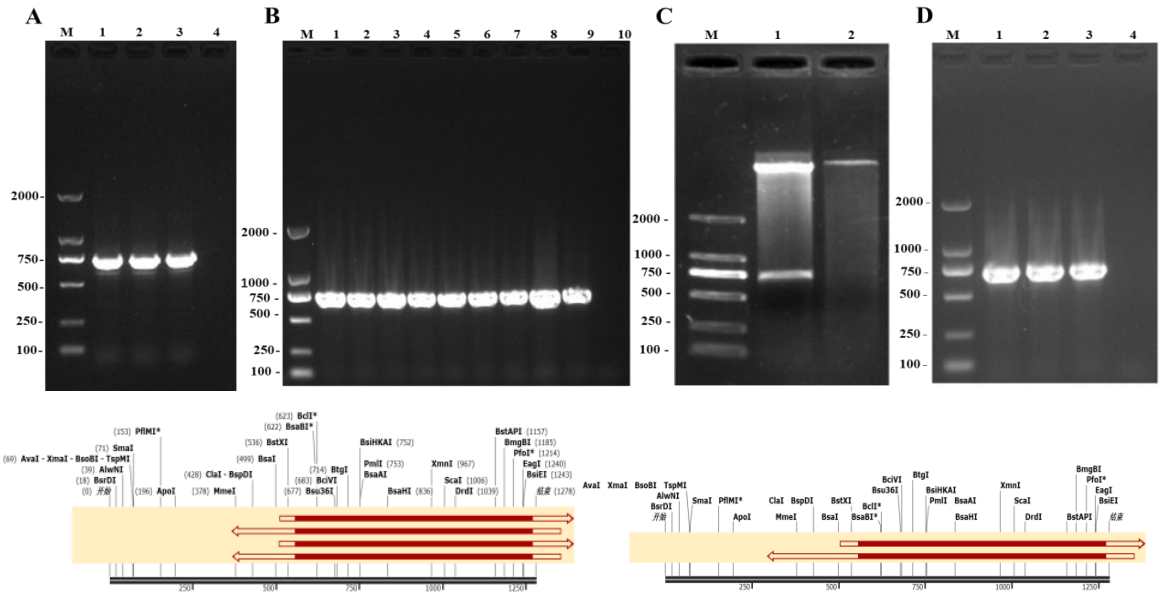

Fig. 2: PCR amplification (A)PCR amplification products (714 bp); (B)Bacterial liquid PCR (clone);(C) Bacterial liquid PCR (expression). (D)Double enzyme digestion identification; (E)Clonal bacterial solution sequencing (F)Expression sequencing of cloned bacterial fluid.

results were obtained with the cloned bacteria solution as shown in Fig. 2(B). Finally, we sequenced the cloned bacterial solution. Fig. 2(2E) performed double enzyme digestion. Fig. 2(C) and expression of the cloned bacterial solution. Fig. 2(D), and finally sequenced the expression. Fig. 2(F). The same bands were obtained in all cases with consistent results.

Prokaryotic Induction, Expression, and Purification of IRF8: In the present experimental procedures, isopropyl β-D-1-thiogalactopyranoside (IPTG) was employed as an inducer to trigger the expression of target proteins in Transetta competent cells. The findings indicated effective induction of the recombinant IRF8 protein, which exhibited a molecular weight of approximately 46 kDa. Following ultrasound treatment, the expressed protein was predominantly found in the form of inclusion bodies as shown in Fig. 3(A, B). We achieved successful solubilization of the recombinant IRF8 protein by employing a urea-based inclusion body lysis buffer as shown in Fig. 3(C). Finally, following purification protocols, the recombinant protein IRF8 was successfully isolated as shown in Fig. 3(D).

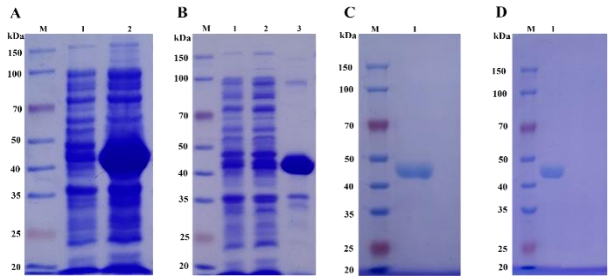

Fig. 3: Construction and induced expression of the recombinant plasmid. (A)Induction of recombinant IRF8 protein. Lane M: Marker (10–150 kDa); Lanes 1–2: with IPTG-induced bacterial protein; (B)Identification of the expression form of recombinant IRF8 protein. Lane M: Marker (10–150 kDa); Lane 1: Sediment of broken bacteria after non induction of expression; Lane 2: supernatant of broken bacteria after induction of expression; Lane 3:Sediment of broken bacteria after induction of expression; (C)Identification of solubility of inclusion bodies. Lane M: Marker (10–150 kDa); Lane 1: precipitation of bacterial fragmentation after induction of expression; (D) Purification results of recombinant IIRF8 protein. Lane M: Marker (10–150 kDa); Lane 1: Purified recombinant IRF8 protein;

Assessment of Antiserum Titers: Enzyme-linked immunosorbent assay (ELISA) was employed to determine the titer of mice anti-chicken IRF8 protein antiserum. The experimental results demonstrated that an antigen coating concentration of 2.5μg/ml yielded the optimal antibody titer. Furthermore, the antibody titer in the group supplemented with *Poria cocos* was significantly higher compared to the group without *Poria cocos*. A titer of 1:409600 for the rabbit anti-chicken IRF8 serum was determined to be appropriate (Fig. 4).

Expression of IRF8 in different tissues: In our experiment, total proteins extracted from 5 tissues were detected by Western blot using a rabbit-derived polyclonal antibody against chicken IRF8. Statistical analysis revealed that, aside from the heart, IRF8 expression was markedly ($P<0.01$) elevated in other tissues, most notably in the lung and pulmonary artery (Fig. 5). In addition, a single clear band appeared in the western blotting results of the polyclonal antibody compared with the negative control, indicating that the antibody had significant specificity against the IRF8 protein expressed in prokaryotic cells (Fig. 5).

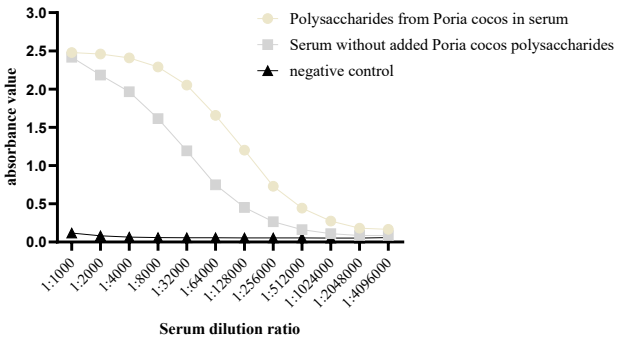

Fig. 4: Serum antibody titer detection (A)The immune time-titer relationship diagram of serum antibodies (dilution ratio 1:100). (B)Detection of serum titer. The yellow is tuckahoe polysaccharide serum;The gray is no added polysaccharide serum; The black is the negative control.

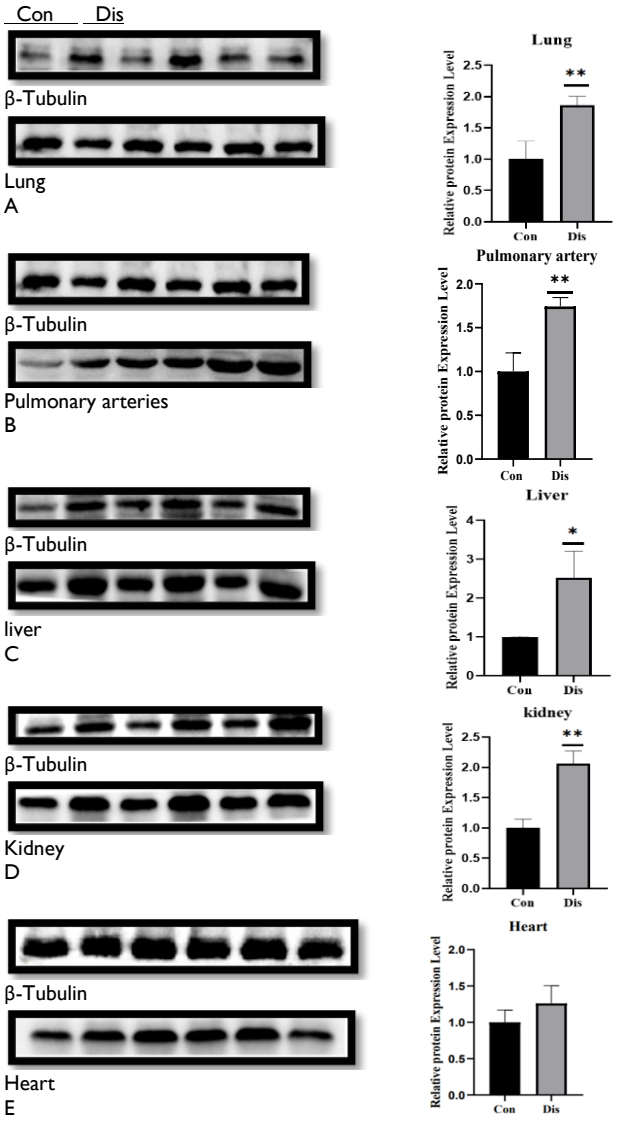

Fig. 5: Protein expression levels of IRF8. (A)Protein expression levels of IRF8 in lungs. (B)Protein expression levels of IRF8 inpulmonary arteries. (C) Protein expression levels of IRF8 in liver. (D)Protein expression levels of T IRF8 in Kidney. (E)Protein expression levels of IRF8 in heart.

The nuclei showed granular brown staining, and the cytoplasm showed diffuse or fibrous staining. The expression of IRF8 in different organs is shown in the Fig. 6. In the ascites group of broilers, the expression level of IRF8 was significantly increased in the pulmonary artery, liver, lung tissue, and kidney; while in the heart tissue, the expression of IRF8 remained stable, which is consistent with the results of the immunofluorescence detection.

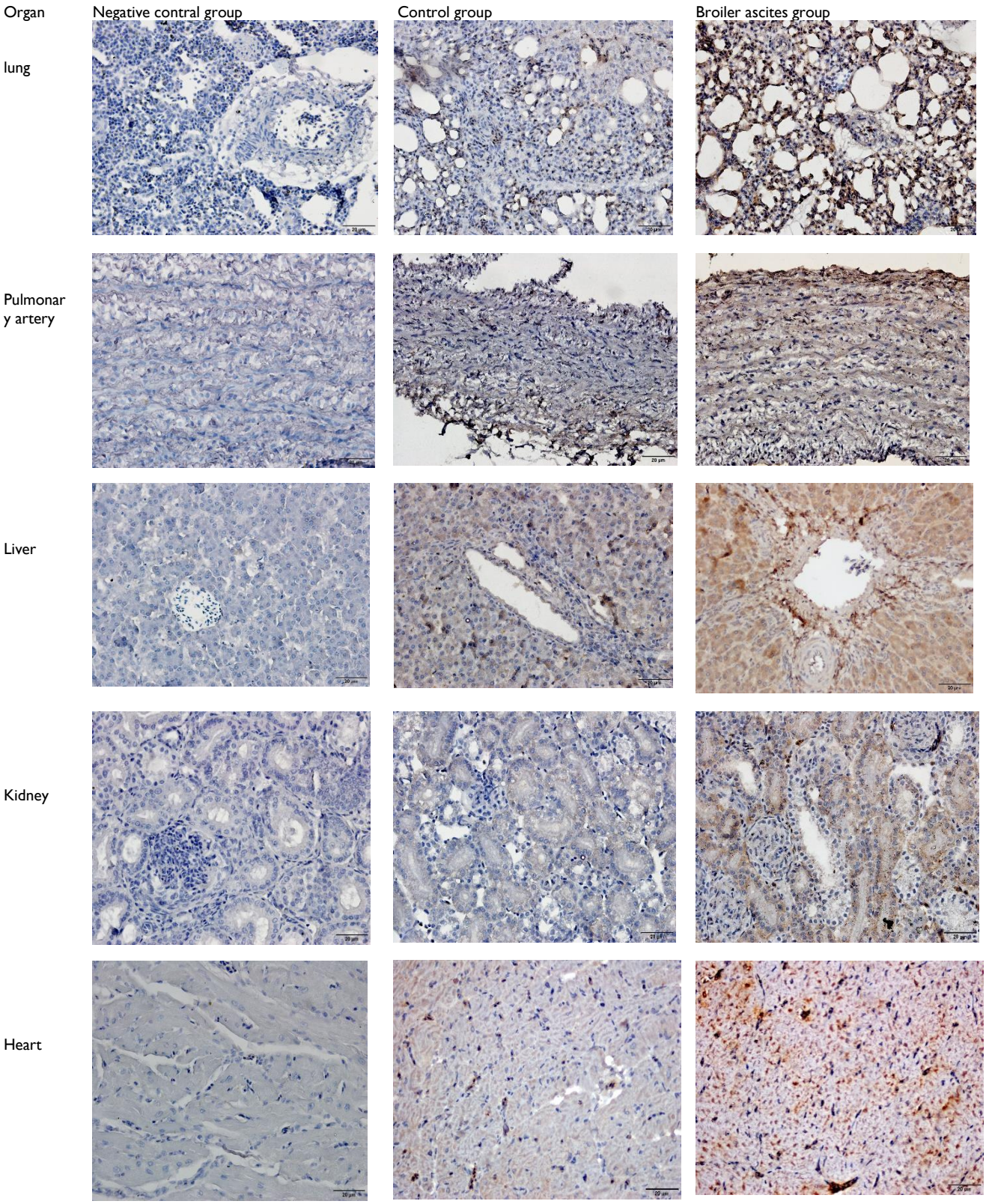

Fig. 6: The expression of IRF8 in the nucleus and cytoplasm of lung, pulmonary artery, liver, kidney and heart in the negative control group, normal group and ascites group. Negative control group: Nearly no brown-positive signals were observed in any tissue, indicating negative expression; Normal control group: A few scattered light brown-positive signals were visible in all tissues, with IRF8 exhibiting low basal expression; Ascites syndrome model group: The intensity and quantity of brown-positive signals were significantly higher in the alveolar walls and interstitium of lung tissue, pulmonary arterial vessel walls, hepatocytes and portal areas of the liver, renal tubular epithelium and interstitium, and cardiac myocytes compared to the previous two groups, with the most pronounced upregulation observed in lung, liver, and heart tissues.

DISCUSSION

In this study, the recombinant IRF8 protein, characterized by its high purity and strong immunogenicity, was successfully generated using an *Escherichia coli* prokaryotic expression system in combination with a PET series vector, and the biological characteristics of the prepared high-quality rabbit anti-chicken IRF8 polyclonal antibody were analyzed (Qiu *et al.,* 2024; Li *et al.,* 2025). As a core member of the interferon regulatory factor family, IRF8 plays a pivotal regulatory role in both innate and adaptive immune responses, and is closely associated with cardiovascular diseases (Ozyigit *et al.,* 2005; Ahmadipour *et al.,* 2018). Currently, research on chicken IRF8 remains relatively scarce, with no systematic reports yet published on the construction of prokaryotic expression systems or the preparation of specific antibodies. The successful completion of this study effectively fills this research gap and lays a foundation for investigating the mechanisms underlying broiler ascites syndrome and developing therapeutic drug targets.

Bioinformatics analysis serves as a prerequisite for target gene cloning and protein expression, with its findings directly guiding the design and optimization of subsequent experimental protocols. In this study, systematic bioinformatics analyses of chicken IRF8 proteins were performed using multiple online tools. Both proteins were found to lack signal peptides and transmembrane domains, indicating they are non-secretory intracellular proteins. This feature is largely consistent with the localization characteristics of their mammalian homologs, suggesting high evolutionary conservation in the subcellular localization of IRF8 across species. It is speculated that, as core immune regulatory proteins, their subcellular localization directly determines the stability of their functional targets and regulatory pathways. The highly conserved localization across species ensures the normal exertion of their key immune regulatory functions, avoiding functional disorders caused by mislocalization, a typical characteristic of functionally conserved proteins in evolution. Hydrophobicity analysis revealed that both proteins are strongly hydrophilic. Their secondary structures are rich in α-helices, β-sheets, and random coils, and contain numerous potential antigenic epitopes. Strong hydrophilicity facilitates the binding of recombinant proteins to immune cell surface receptors and triggers immune responses. Meanwhile, abundant α-helices, β-sheets, and random coils form stable and complex spatial conformations, providing structural foundations for the formation of potential antigenic epitopes, which in turn can effectively stimulate the production of specific antibodies.

The construction and optimization of prokaryotic expression systems are critical steps for obtaining highly active and high-yield recombinant proteins. The adaptability of prokaryotic expression systems directly determines the transcription and translation efficiency of the target gene, the proper folding of the recombinant protein, and the preservation of its activity, serving as the pivotal link between target gene cloning and recombinant protein purification. For this study, namely pEASY-T3 and pET-32a (+), were chosen for gene cloning and protein expression in this experiment. The results show that when we perform cloning and recombination, the recombination efficiency is very high. Research demonstrates *Escherichia coli* expression systems exhibit distinct strengths over alternatives, including well-defined genetic profiles, robust sustained fermentation capacity, and minimal environmental requirements (Varmaghany *et al.,* 2015). Literature shows that the T terminal carried by the T3 vector at the 3 'end of each chain can complement and pair with the a terminal of PCR cloned products, quickly, accurately, and efficiently improving the ligation and cloning efficiency of PCR products. In our experimental work, the pET-32a(+) plasmid was selected as the expression vector, which facilitated the successful prokaryotic expression induction and subsequent purification of the recombinant IRF8 protein(Saeki *et al.,* 2024). Research evidence shows that the pET-32a (+) system contains a T7 promoter and a pair of His tags, which collectively make it highly suitable for protein expression experiments in *Escherichia coli*. (Akhlaghi *et al.,* 2012). Through its interaction with inserted foreign genes, this system enables the production of substantial quantities of soluble, biologically active protein. Ultimately, a recombinant IRF8 protein of high purity and concentration was successfully isolated (Antanasijevic *et al.,* 2021; Yi *et al.,* 2022). In our experimental design, the Trans5α strain was selected as the cloning host to integrate exogenous genetic sequences, while the DE3 strain served as the expression host for protein synthesis. This dual-strain strategy significantly enhanced the purification efficiency of the recombinant protein, resulting in a substantial yield of soluble and biologically active protein molecules.

In this study, the recombinant IRF8 protein was predominantly expressed in the form of inclusion bodies. After urea dissolution, nickel affinity chromatography, and gradient imidazole elution, high-purity protein products were successfully obtained, which provided high-quality antigens for subsequent antibody preparation. The titer and specificity are the core indicators for the application of polyclonal antibodies (Lanca *et al.,* 2022; Li *et al.,* 2024). In the present study, New Zealand white rabbits were selected as immunized animals, and high-titer and high-specificity antibodies were acquired after five rounds of immunization. The results showed that the antiserum titer reached 1:2,048,000. A single distinct band was detected via Western blot, which verified the rationality of the immunization procedure and the favorable immunogenicity of the recombinant protein. IHC results showed increased positive staining intensity and area of IRF8 in various tested tissues of broilers in the AS model group. Western blot analysis confirmed that compared with the normal control group, IRF8 expression was extremely significantly upregulated in the pulmonary artery, kidney, lung, and significantly upregulated in the liver and heart of the AS model group, indicating a close association between IRF8 upregulation and AS pathogenesis, with tissue-specific regulatory effects (Tamura *et al.,* 2015; Nixon *et al.,* 2022). AS is closely associated with abnormal immune-inflammatory responses. As a core immune regulatory factor, IRF8 modulates immune-inflammatory responses by regulating the development and differentiation of immune cells and

the release of inflammatory cytokines (Moorman *et al.,* 2022). The extremely significant upregulation of IRF8 in the pulmonary artery may promote vascular constriction and thickening by regulating vascular wall inflammation, thereby contributing to the development of pulmonary hypertension, which is consistent with its central role in inflammatory regulation.

Moreover, as a transcription factor, IRF8 upregulation may activate downstream immune-inflammatory-related target genes to amplify inflammatory responses and exacerbate tissue injury. Previous studies have demonstrated that aberrant IRF8 expression disrupts immune homeostasis and is involved in the pathogenesis of autoimmune diseases (Rahimi *et al.,* 2023).

Conclusions: To summarize, this research successfully produced polyclonal antibodies targeting IRF8 through the prokaryotic expression of the recombinant IRF8 protein followed by animal immunization. The results indicate that IRF8 could function as a specific biomarker for AS and might represent a promising selective target in the development of anti-AS therapeutics. These experimental outcomes offer a useful reference for generating IRF8 polyclonal antibodies and establish a basis for deeper investigation into the interaction mechanisms between IRF8 and AS.

Acknowledgment: This work was financially supported by the Regional Program of the National Natural Science Foundation of China (Grant No. 32460906), the General Program of the Natural Science Foundation of Jiangxi Province (Grant No. 20224BAB20503), and the Key Program of the Science and Technology Research Project of Jiangxi Provincial Department of Education (Grant No. GJJ2200406); the Science and Technology Research Project of Jiangxi Provincial Department of Education (No.191400).

Authors Contribution: SC, PL and GH conceived and designed the review. LL, XL, XH conducted the experimental procedures and examined the serum and tissue specimens. XG, XG, and PL performed the data analysis. Every author contributed to interpreting the findings, provided critical revisions to the manuscript for significant intellectual content, and gave their approval to the definitive version.

Disclosures: These authors declare that they have no conflicts of interest to disclose.

REFERENCES

Ahmadipour B, Sharifi M and Khajali F, 2018. Pulmonary hypertensive response of broiler chickens to arginine and guanidinoacetic acid under high-altitude hypoxia. Acta Veterinaria Hungarica 66(1):116-124. https://doi.org/10.1556/004.2018.011

Antanasijevic A, Sewall L M, Cottrell C A, *et al.,* 2021. Polyclonal antibody responses to hiv env immunogens resolved using cryoem. Nature Communications 12(1):4817. https://doi.org/10.1038/s41467-021-25087-4

Cytlak U, Resteu A, Pagan S, *et al.,* 2020. Differential irf8 transcription factor requirement defines two pathways of dendritic cell development in humans. Immunity 53(2):353-70. https://doi.org/10.1016/j.immuni.2020.07.003

Daneshyar M, Kermanshahi H and Golian A, 2009. Changes of biochemical parameters and enzyme activities in broiler chickens with cold-induced ascites. Poultry Science 88(1):106-110. https://doi.org/10.3382/ps.2008-00170

Habibian M, Sadeghi A and Karimi A, 2025. Dietary methanol extract of purslane (*portulaca oleracea l.*) can help reduce the negative impacts of triiodothyronine-induced ascites in broiler chickens. Veterinary Research Communications 49(3):147. https://doi.org/10.1007/s11259-025-10723-x

Lanca T, Ungerback J, Da S C, *et al.,* 2022. Irf8 deficiency induces the transcriptional, functional, and epigenetic reprogramming of cdc1 into the cdc2 lineage. Immunity 55(8):1431-47. https://doi.org/10.1016/j.immuni.2022.06.006.

Li L, Jia Q, Chen L, *et al.,* 2022. Changes in the expression of mif and other key enzymes of energy metabolism in the myocardia of broiler chickens with ascites syndrome. Animals 12(19): https://doi.org/10.3390/ani12192488

Li N, Steiger S, Zhong M, *et al.,* 2024. IRF8 maintains mononuclear phagocyte and neutrophil function in acute kidney injury. Heliyon 10(11):e31818. https://doi.org/10.1016/j.heliyon.2024.e31818

Li X, Zhang H, Yu F, *et al.,* 2025. IRF8 aggravates nonalcoholic fatty liver disease via bmal1/ppargamma axis. Genes and Diseases 12(3):101333. https://doi.org/10.1016/j.gendis.2024.101333

Liang K L, Laurenti E and Taghon T, 2023. Circulating IRF8-expressing CD123(+)CD127(+) lymphoid progenitors: key players in human hematopoiesis. Trends in Immunology 44(9):678-92. https://doi.org/10.1016/j.it.2023.07.004

Liu P, Yang F, Zhuang Y, *et al.,* 2017. Dysregulated expression of microRNAs and mRNAs in pulmonary artery remodeling in ascites syndrome in broiler chickens. Oncotarget, 8(2):1993-2007. https://doi.org/10.18632/oncotarget.12888

Moorman HR, Reategui Y, Poschel D B, *et al.,* 2022. IRF8: Mechanism of action and health implications. Cells 11(17): https://doi.org/10.3390/cells11172630

Nixon B G, Kuo F, Ji L, *et al.,* 2022. Tumor-associated macrophages expressing the transcription factor IRF8 promote T cell exhaustion in cancer. Immunity 55(11):2044-58. https://doi.org/10.1016/j.immuni.2022.10.002

Ozyigit MO, Kahraman MM and Sonmez G, 2005. The identification of matrix metalloproteinases and their tissue inhibitors in broiler chickens by immunohistochemistry. Avian Pathology 34(6):509-16. https://doi.org/10.1080/03079450500368508

Peng W, Fang W, Gao X, *et al.,* 2024. Effect of RNA interference with hif-1alpha on the growth of pulmonary artery endothelial cells in broiler chickens. Poultry Science 103(5):103388. https://doi.org/10.1016/j.psj.2023.103388

Qiu Z, Khalife J, Ethiraj P, *et al.,* 2024. IRF8-mutant B cell lymphoma evades immunity through a cd74-dependent deregulation of antigen processing and presentation in MHCII complexes. Science Advances 10(28):eadk2091. https://doi.org/10.1126/sciadv.adk2091

Rahimi M, Rahimi S, Karimi TM, *et al.,* 2023. Peroxisome proliferator-activated receptor gamma (PPARgamma) activation: A potential treatment for ascites syndrome in broiler chickens. Poultry Science 102(9):102859. https://doi.org/10.1016/j.psj.2023.102859

Shi S, Shen Y, Zhang S, *et al.,* 2017. Combinatory evaluation of transcriptome and metabolome profiles of low temperature-induced resistant ascites syndrome in broiler chickens. Scientific Reports 7(1):2389. https://doi.org/10.1038/s41598-017-02492-8

Tamura T, Kurotaki D and Koizumi S, 2015. Regulation of myelopoiesis by the transcription factor irf8. International Journal of Hematology, 101(4):342-51. https://doi.org/10.1007/s12185-015-1761-9

Varmaghany S, Karimi T M, Rahimi S, *et al.,* 2015. The effects of increasing levels of dietary garlic bulb on growth performance, systolic blood pressure, hematology, and ascites syndrome in broiler chickens. Poultry Science 94(8):1812-20. https://doi.org/10.3382/ps/pev148.

Yi X, Wang Z, Xiong X, *et al.,* 2022. Preparation and characterization of a polyclonal antibody against pten-long. Biotechnology and Applied Biochemistry 69(4):1622-32. https://doi.org/10.1002/bab.2232

Zohrabi M, Khajali F and Dastar B. 2024. Effect of barley processing and enzyme supplementation on broiler performance, gut morphometry, and the occurrence of ascites syndrome in broiler chickens. Poultry Science 103(12):104410. https://doi.org/10.1016/j.psj.2024.104410